Rapid feature selective neuronal synchronization through correlated latency shifting

Pascal Fries[1, 2, 3], Sergio Neuenschwander[1], Andreas K. Engel[1,4], Rainer Goebel[1,5] and Wolf Singer[1]

[1] *Max-Planck Institute for Brain Research, Deutshcordenstraße 46, 60528 Frankfurt am Main, Germany*

[2] *Johann Wolfgang Goethe-University, Department of Psychiatry, Heinrich-Hoffmann Straße 10, 60528 Frankfurt am Main, Germany*

[3] *Present address: Laboratory of Neuropsychology, National Institute of Mental Health, Building 49, 49 Convent Drive, MSC 4415, Bethesda, Maryland 20892, USA*

[4] *Present address: Research Centre Juelich, Institute for Medicine, Cellular Neurobiology Group, 52425 Juelich, Germany*

[5] *Present address: University of Maastricht, Neurocognition Group, Department of Psychology, Postbus 616, 6200 MD Maastricht, The Netherlands*

Correspondence should be addressed to W.S. (singer@mpih-frankfurt.mpg.de)

Spontaneous brain activity could affect processing if it were structured, . We show that neuron pairs in cat primary visual cortex exhibited correlated fluctuations in response latency, particularly when they had overlapping receptive fields or similar orientation preferences. Correlations occurred within and across hemispheres, but only when local field potentials (LFPs) oscillated in the gamma-frequency range (40–70 Hz). In this range, LFP fluctuations preceding response onset predicted response latencies; negative (positive) LFPs were associated with early (late) responses. Oscillations below 10 Hz caused covariations in response amplitude, but exhibited no columnar selectivity or coordinating effect on latencies. Thus, during high gamma activity, spontaneous activity exhibits distinct, column-specific correlation patterns. Consequently, cortical cells undergo coherent fluctuations in excitability that enhance temporal coherence of responses to contours that are spatially contiguous or have similar orientation. Because synchronized responses are more likely than dispersed responses to undergo rapid and joint processing, spontaneous activity may be important in early visual processes.

The cerebral cortex is spontaneously active, and the excitability of its neurons fluctuates[1]. As a consequence, responses of visual cortex neurons to successively presented, physically unchanged stimuli vary in both amplitude and latency[2,3]. Generally, these fluctuations are considered to result from noise and hence, to be uncorrelated[4]. In neurophysiological studies, the fluctuations of single-cell responses are eliminated by extensive averaging across successive trials; the nervous system has been proposed to cope with this variability by averaging across large populations of neurons tuned to the same features[4]. However, these spontaneous fluctuations of neuronal excitability may not be uncorrelated but may exhibit specific spatiotemporal patterning. In that case, spontaneous activity could be important in signal processing. Coordinated excitability changes could produce correlated fluctuations of response latencies, thereby increasing the temporal coherence of selected subsets of neuronal responses. Because synchronous responses have a stronger influence on cells in target structures than temporally dispersed responses[5,6] (for review, see ref. 7), coordinating response latencies could be effective in rapidly grouping responses for further joint processing. If such latency covariations exhibited topological specificity, they could effectively contribute to fast, feature specific binding of responses such as is required for perceptual grouping and scene segmentation. Moreover, if the spontaneously occurring fluctuations in response latency and amplitude are not random but exhibit specific correlation patterns, it should be reconsidered whether neuronal processes are really as noisy as commonly assumed, and whether averaging across large populations of neurons is effective for noise reduction. If spontaneous fluctuations were correlated, noise reduction by averaging would be inefficient, and if those fluctuations contain information, averaging might even be inappropriate.

In a previous study[8], voltage-sensitive dye imaging was combined with single-cell recordings to show that spike-triggered averages of the images exhibited a columnar pattern whereby the orientation preference of the active columns matched that of the recorded neuron. This suggests that spontaneous fluctuations in excitability are correlated within and across columns with similar orientation preference. With multielectrode recordings, we show that these spontaneous fluctuations affect response latencies and amplitudes and in particular, that they can enhance the temporal coherence of light responses in a feature-selective way. However, this only occurs when the cortex is in an activated state and spontaneous excitability changes fluctuate in the gamma frequency range, the range around 40 Hz.

Results

With multielectrodes, we recorded from neurons in the cat visual cortex. The intertrial variance of latencies of responses to stationary flashed light stimuli was considerable (Fig. 1). When averaged across all recording sites, the mean latency variance was 31.6 ± 1.3 ms^2 (mean ± s.e.m., $n = 212$), whereas the mean latency was 48.1 ± 0.93 ms. To examine whether the latencies of responses

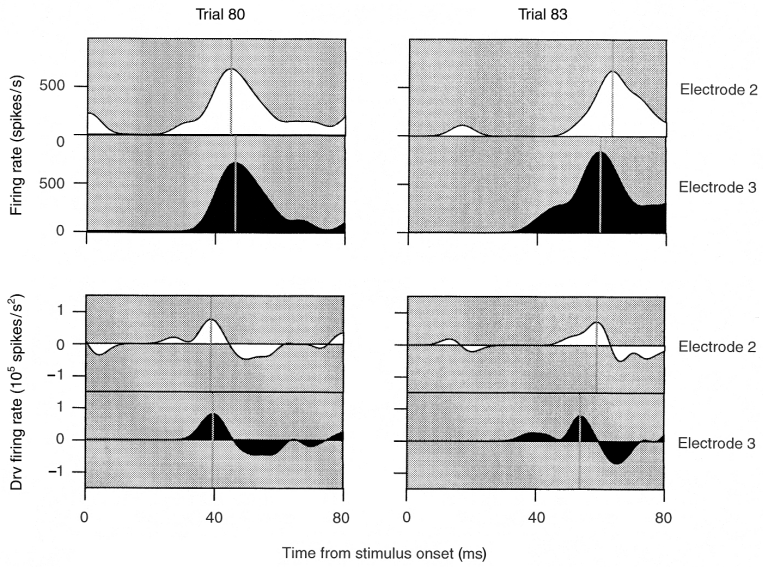

Fig. 1. Determination of response onset latencies. Time course of spike density functions (firing rate) and their derivatives (drv firing rate) computed from responses of electrode 2 (white) and 3 (black) for two different stimulus presentations (trials 80 and 83). Vertical lines, latencies as determined from the peaks of the spike density functions or their derivatives. Latency relationships assessed by the two measures are similar.

recorded simultaneously from different sites covaried, we calculated Spearman rank correlations between the latencies from different sites. A positive correlation value indicated that neurons at one recording site responded earlier than average when the neurons at the second recording site responded early, and vice versa (example, Fig. 2). Of 392 pairs, 98 (25%) showed significant positive correlations ($p < 0.05$, Spearman rank correlation) with a mean correlation coefficient (r) of 0.34 ± 0.0095 (mean ± s.e.m., range, 0.18–0.55, Fig. 3a). Only one pair showed a significant negative correlation ($r = –0.25$). The overall distribution was significantly above zero ($p < 0.0001$, sign test).

These latency covariations cannot be attributed to uncontrolled fluctuations in stimulus timing or intensity, because control measurements with a photodiode confirmed submillisecond precision of stimulus onset and the lack of contrast changes (data not shown). It is also unlikely that covariations resulted from changes in the multi-neuron composition. Latency covariations occurred on a trial-by-trial basis (Figs. 1 and 2), but stimuli were identical across trials. Systematic and coherent, trial locked changes of multi-neuron composition are thus improbable. Nor could latency covariations be attributed to shared thalamic input because they existed for neuronal responses recorded from different hemispheres (Fig. 4). Average latency correlations were as strong for interhemispheric as for intrahemispheric pairs ($p > 0.6$, Mann-Whitney U test) and significantly above zero in both cases (sign tests, interhemispheric, $p < 0.002$, $n = 74$; intrahemispheric, $p < 0.002$, $n = 57$; Fig. 3c).

To control for the possibility that latency covariations are due to global excitability fluctuations like those that are associated with highly synchronized brain rhythms and that occur during sleep or anesthesia, we recorded from area V4 of an awake fixating macaque monkey. Twelve of the 32 pairs of recording sites (38%) showed a significantly positive latency correlation ($p < 0.05$, 0.27 ± 0.05, mean ± s.e.m., range, 0.13–0.68). There was no significant negative latency correlation. As in the cat, the overall distribution was significantly above zero ($p < 0.0001$, sign test, Fig. 3b). Thus, latencies were often correlated in the visual cortex of the awake and atten-

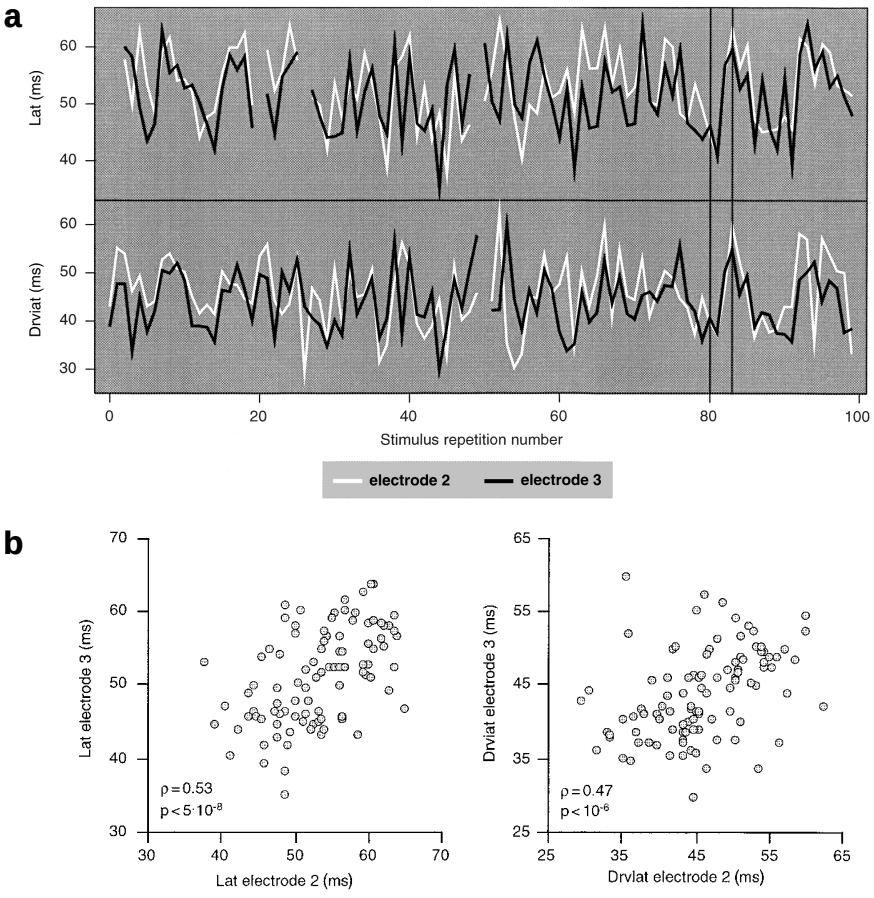

Fig. 2. Covariation of latencies. (**a**) Response latencies (ordinate) derived from spike density functions (lat) and their derivatives (drvlat) of the same neurons as in Fig. 1, for 100 successive stimulus repetitions (abscissa). Gaps correspond to trials for which latencies could not be determined. Two vertical lines, responses shown in Fig. 1. (**b**) Latencies derived from the spike density functions (left) and their derivatives (right) recorded from electrodes 2 (x-axis) and 3 (y-axis).

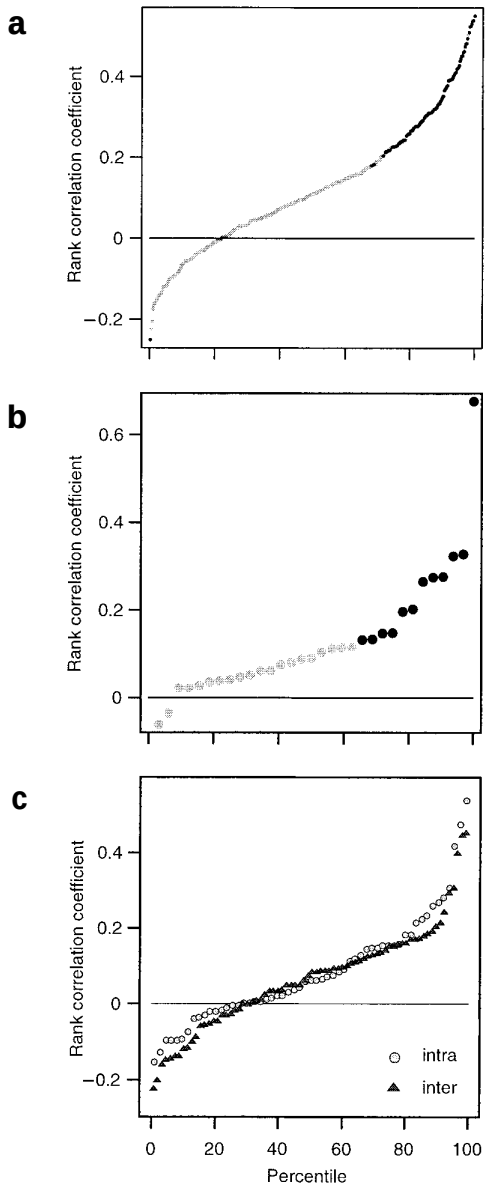

Fig. 3. Distributions of latency correlations. (**a**) Percentile plot of correlation coefficients (for peak latencies) of all 392 intrahemispheric pairs of recording sites in the cat. Black dots indicate significant correlations. (**b**) Same distribution for data from the awake macaque monkey (n = 32). (**c**) Rank correlation coefficients for all simultaneously recorded intrahemispheric (gray circles) and interhemispheric (black triangles) pairs of recording sites. Although both distributions were significantly above zero, there was no significant difference between them.

tively fixating macaque monkey and therefore could not be caused by brain rhythms that occurred only during sleep or anesthesia.

Subthreshold membrane potential fluctuations influence spike timing, as demonstrated by both *in vitro*[9–13] and *in vivo* studies[14], and can be highly correlated over both short[15] and long[16] cortical distances. If latency shifts are caused by fluctuations of membrane potential that are synchronous in local clusters of cells, one should be able to predict latencies from the trajectories of LFP fluctuations preceding the onset of responses. This is because LFPs reflect the average transmembrane currents of neurons in a volume of several hundred microns radius around the electrode tip[17]. To examine the relationship between LFP fluctuations and response latency, we compared LFP trajectories at one recording site with response latencies at the other. We restricted this analysis to interhemispheric recordings to minimize cross-talk through volume conduction and to avoid any circularity that might arise by evaluating LFPs and spikes recorded from the same electrode. Sorting responses according to LFP trajectories preceding response onset revealed that negative (positive) LFPs predicted short (long) latencies ($p < 0.0001$, $n = 180$, paired sign-test; Fig. 5). This agrees with the notion that negative LFPs correspond to intracellular depolarization[17]. Prediction of response latencies from LFP trajectories was possible as early as 16 ms after stimulus onset, excluding the possibility that the LFP trajectories were themselves influenced by responses to the stimulus; but no predictions on response latency were possible over intervals longer than 20 ms. These results indicate that the coherent fluctuations of response latencies are due to synchronous fluctuations of the membrane potential of local groups of neurons that are correlated both within as well as across hemispheres. The limitation of predictability to intervals as short as 20 ms suggests that these excitability fluctuations occurred at a fast time scale, in the frequency range of gamma oscillations.

If latency covariations result from rapid rather than slow fluctuations of the membrane potential, then they should be particularly pronounced if LFP oscillations exhibit high-frequency components. We calculated for all pairs of recording sites the average cross-power spectrum of the LFPs (recorded from the same electrodes as the spikes; see Methods) in the one-second period preceding stimulus onset. The cross-power spectrum estimates the frequency content common to both signals. A highly significant positive correlation occurred between the precision of latency covariations and the amount of LFP power in the gamma frequency range (38 to 68 Hz, Spearman rank correlation; Fig. 6a). Because an increase of power in the high frequencies is associated with a decrease in power in the low-frequency range, this correlation was negative for power in the low range (9 to 18 Hz). Thus, coordinated fluctuations of response latencies occur preferentially during states characterized by high gamma activity.

To examine the effect on absolute latencies of gamma power before the stimulus, we calculated the Spearman rank-correlation between the auto-power spectra of the ongoing LFPs, and the median latencies for all 212 recording sites for which we were able to determine latencies (Fig. 6b). We found that response latencies are on average longer when LFP oscillations are in the low- (1–10 Hz) rather than the high-frequency range (20–70 Hz). However, this effect cannot account for the latency covariations occurring with high gamma power for the following reasons. First, the non-parametric Spearman rank-correlation test is independent of absolute latencies, and second, the dependence of latency fluctuations on preceding LFP trajectories (Fig. 5) indicates that the latency changes leading to significant covariance occurred on a much faster time scale than the slow and state-dependent drifts in the frequency composition of the LFP.

Shortening of absolute latencies could have resulted from shortened period length of membrane potential fluctuations, as this reduces maximal delays[10], or it could have been due to increased global excitability during phases of high gamma. If the latter had been the case, one should expect enhanced discharge rates in responses preceded by high gamma activity (Fig. 6d, same analysis as in Fig. 6b for peak firing rates versus pre-stimulus auto-power of the LFP). Only power in frequencies below 5 Hz predicts high firing rates, whereas power in frequencies above 10 Hz predicts reduced peak firing. Overall, the peak firing rates show only weak

correlation with pre-stimulus LFP power. Thus, short latencies during enhanced gamma activity are most likely not due to globally enhanced excitability.

In conclusion, during states characterized by high gamma activity, absolute response latencies shorten, and the light responses of a significant fraction of cortical neurons exhibit rapid and coherent fluctuations of their latencies. To determine whether these coherent fluctuations are global, or exhibit columnar selectivity, we analyzed latency covariance as a function of the spatial overlap and the orientation preference of the neurons' receptive fields (RFs). For pairs with overlapping RFs, the strength of latency covariation was positively correlated with the amount of RF overlap ($r = 0.12$, $p < 0.05$, $n = 271$). For pairs with non-overlapping RFs and significant orientation selectivity, the strength of latency covariations was positively correlated with the degree of orientation preference similarity ($r = 0.28$, $p < 0.05$, $n = 55$); this was not the case for pairs with overlapping RFs ($r = –0.006$, $p = 0.95$, $n = 129$). This indicates that the coherence of spontaneous excitability fluctuations exhibits topological specificity, and the specific pattern of coherent fluctuations suggests intracortical interactions[18] as a cause, because it matches precisely the topology of tangential intra-areal and of callosal connections[19,20].

We have identified high RF overlap and high prestimulus LFP gamma power as the predictors of the strongest latency correlations. Because the average latency correlation across all pairs of recording sites was only 0.34, we selected subsets of recording site pairs using these predictors of strong correlations as selection criteria. We calculated average latency correlations in these subsets to arrive at an estimate of correlation strength among responses whose grouping would be meaningful in the context of perceptual binding. Prestimulus LFP components of 44 to 56 Hz had a par-

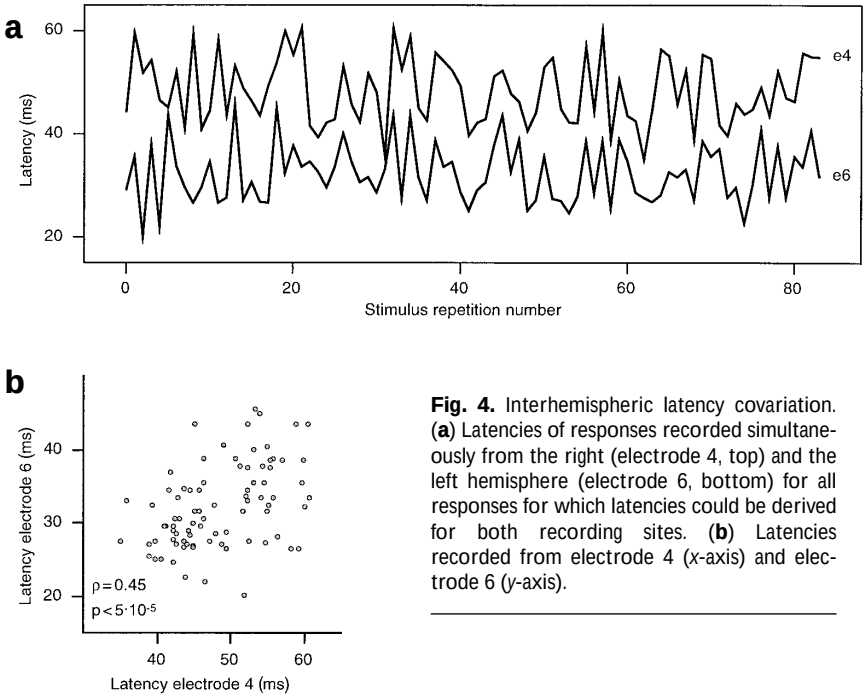

Fig. 4. Interhemispheric latency covariation. (**a**) Latencies of responses recorded simultaneously from the right (electrode 4, top) and the left hemisphere (electrode 6, bottom) for all responses for which latencies could be derived for both recording sites. (**b**) Latencies recorded from electrode 4 (*x*-axis) and electrode 6 (*y*-axis).

Fig. 5. Prediction of spike response latencies by LFP phase. (**a**) Top, averaged LFPs ($n = 25$, thickness, ± s.e.m.) whose trajectories fall (black, negative going) or rise (gray, positive going) in the interval preceding response onset. Response onset (right vertical line) was determined from the grand average of all LFPs (thin trace), which corresponds to the visual evoked potential. For the averages shown as black and gray curves, LFPs were selected that exhibited maximal rates of change just before response onset. The first vertical line indicates the first bin after stimulus onset in which the two LFPs started to differ significantly (*t*-test, $p < 0.05$). The LFP averages start to bifurcate about 10 ms before response onset. LFPs were recorded from a site in the left hemisphere. Bottom, responses of neurons recorded from a site in the right hemisphere that exhibited significant latency covariations with neurons at the site in the left hemisphere from which the LFPs in (**a**) were recorded. Traces show averages (± s.e.m.) of firing rates calculated separately for trials with falling (black) and rising (gray) LFPs as defined in (**a**). Responses preceded by negative (positive) going LFPs have short (long) latencies. (**b**) Spike response latencies as a function of LFP trajectories for all interhemispheric recording pairs. *x*-axis, LFP falling; *y*-axis, LFP rising. The majority of dots are located above the diagonal.

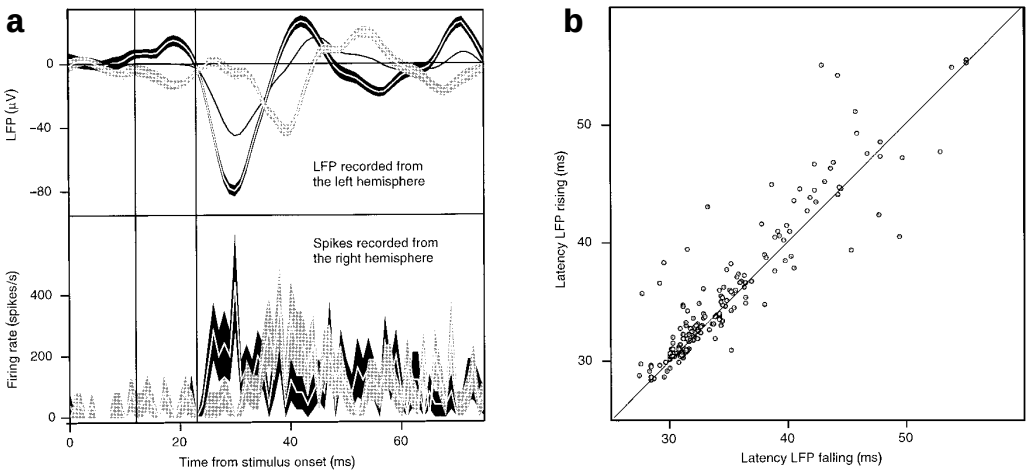

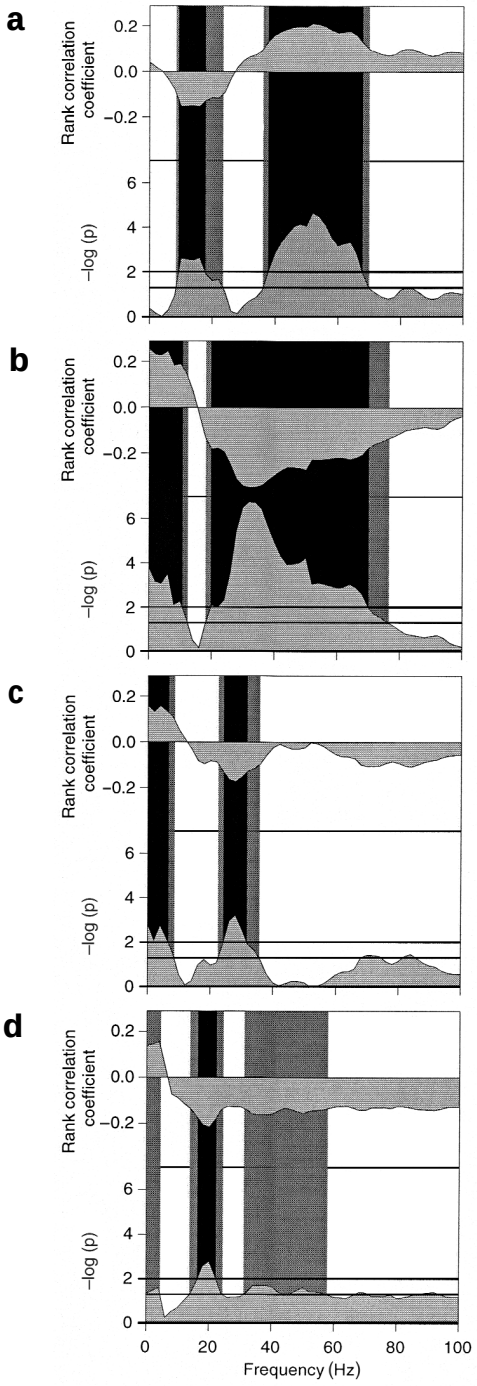

Fig. 6. Influence of prestimulus LFP power on latencies, firing rates and their correlations. (**a**) Binwise (2 Hz/bin) rank correlation between the cross-power spectra of the ongoing LFPs and the latency correlation for 392 pairs of recording sites. Top, Spearman's rank correlation coefficient. Bottom, negative logarithm to the base 10 of the two-sided significance of the rank correlation. Horizontal lines in lower graph are drawn at 5% (bottom line) and 1% (top line) significance levels. Frequencies for which we found significant (highly significant) latency correlations are underlaid with gray (black) shading. (**b**) Binwise (2 Hz/bin) rank correlation between the auto-power spectra of the ongoing LFPs and the median latency for 212 recording sites. Conventions as in (**a**). (**c**) Same analysis as in (**a**) for relationships between cross-power and covariations in peak firing rate (n = 392). (**d**) Same analysis as in (**b**) for correlations between auto-power and peak firing rates (n = 212).

ticularly strong correlation with latency covariation (Fig. 6a). Therefore, we first selected those pairs of recording sites for which the power in the 44 to 56 Hz range was in the upper 10% of the respective distribution. From the 40 pairs in the high gamma group, 17 (43%) showed significant latency correlations with an average strength of 0.41. This is an increase of 72% (from 25%) in the frequency of significant correlations and an increase by 21% (from 0.34) in the average strength when compared to the unselected population. Selecting from the high gamma group, those pairs (n = 2) that were in the upper 10% of the distribution of RF overlap also revealed strong correlations. One of 2 pairs meeting these criteria showed a significant latency correlation with a strength of 0.45 (an increase by 32%). As some pairs of recording sites not belonging to these selected subsets also exhibited strong latency correlations, further unknown factors likely influence the probability of latency correlations.

It is commonly held that coherence of cortical excitability fluctuations is particularly pronounced when the EEG is synchronized, that is, when it exhibits low-frequency oscillations of large amplitude[21]. This raises the question of why, in the present study, latency covariations were measurable only when the EEG was desynchronized and exhibited high gamma power. One possibility is that the slow fluctuations of membrane potential associated with low-frequency EEG do not sufficiently focus responses to the peaks of the oscillations to generate significant covariations of response latencies[11]. To examine this possibility, we also measured fluctuations of peak response amplitudes (see Methods). Of 392 pairs, 131 (33%) showed significant positive correlations ($p < 0.05$, Spearman rank correlation) with a mean correlation coefficient of $r = 0.39 \pm 0.01$ (mean ± s.e.m., range, 0.18–0.78). Only one pair showed a significantly negative correlation ($r = -0.31$). A dissociation between latency and amplitude covariations occurred when amplitude covariations were assessed as a function of prestimulus local field potential power (Fig. 6c). Although prestimulus gamma power predicted strong latency covariations (Fig. 6a), it did not have a significant influence on amplitude covariations (Fig. 6c). Only frequency components below 10 Hz showed a weak significant positive correlation to amplitude covariations. However, these amplitude covariations failed to exhibit significant relations with the orientation preferences of the respective cells (Spearman rank correlations, $r = -0.03$, $p > 0.7$, n = 129 for all pairs; $r = -0.08$, $p > 0.5$, n = 55 for pairs with non-overlapping RFs). Only receptive field overlap showed a relationship to amplitude covariation ($r = 0.17$, $p < 0.01$, n = 271). This suggests that the fluctuations of excitability that are associated with high gamma power in the LFP and that lead to latency covariations are too fast to generate coherent rate fluctuations. Conversely, the excitability fluctuations associated with low- frequency LFPs, which seem to be too slow to cause significant latency correlations, led to clear covariations of response amplitudes. The data suggest further that the slow fluctuations exhibit much less topological selectivity and are of a more global nature than the fast fluctuations because the rate covariations failed to exhibit columnar selectivity for orientation preference. Optical recordings show that neurons in the visual cortex have a heightened probability of generating a spontaneous spike when neurons in other columns showing the same orientation preference are active as well[8]. This agrees with the latency data, as it indicates that spontaneous excitability fluctuations can exhibit columnar selectivity. However, our data suggest that column-specific covariations of excitability may be confined to states characterized by high gamma power and may then enhance the coherence of responses to visual stimuli mainly by adjusting the timing of responses on a fast time scale rather than by modulating response amplitudes.

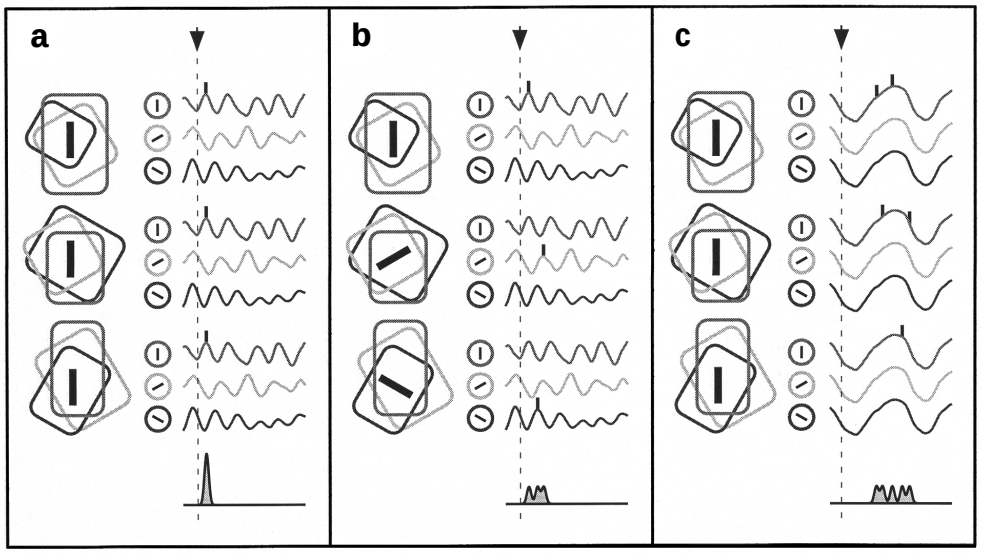

Fig. 7. Rapid feature-selective neuronal synchronization through correlated latency shifting. (**a**) Three groups of neurons (circles) with differing orientation preferences (indicated by bars) and RFs at three different locations in the visual field (left column). LFPs reflecting membrane potential fluctuations (right) oscillate in the gamma frequency range and are coherent for neurons with the same and incoherent for neurons with different orientation preference. A stimulus array of three vertical bars (black bars over the RFs) drives neurons selective for vertical orientations (time of EPSP arrival indicated by arrow and dotted line). Response onsets are shifted coherently due to coherent membrane potential fluctuations, leading to a well synchronized population response, as indicated by the sharp spike density function (bottom). For simplicity, effects of RF overlap are not considered. (**b**) Same conventions as in (**a**), but stimulation with bars of different orientations. As the membrane potentials of the activated neurons fluctuate incoherently, response onsets are not synchronized and lead to a temporally dispersed population response. (**c**) Same stimulation condition as in (**a**) but the LFPs now oscillate at low frequency and are coherent for all groups of neurons. Due to their low frequency, the membrane potential oscillations have no latency-shifting effect. Neurons fire more spikes than with gamma-dominated LFP (**a**), but latencies are longer, and responses are spread out in time. In this case, responses to non-aligned bars would exhibit the same temporal dispersion as the responses to aligned bars.

Discussion

Modulating the temporal coherence of responses could be used for rapid response selection and grouping. Synchronized responses have a stronger influence on cells at subsequent processing stages than do non-synchronized responses[5–7]. Thus, synchronized responses are transmitted more rapidly and reliably[22], and because of jointly enhanced saliency, have a higher probability of being processed together. Spontaneous activity could thus serve to continuously translate the functional architecture of cortico–cortical association connections into coherent and column-specific excitability fluctuations. These, in turn, could bias the grouping of responses to afferent signals by adjusting their temporal coherence (Fig. 7). Such a mechanism has several advantages. First, grouping can be achieved faster if the exchange of signals through cortico–cortical connections does not start only once cells begin to respond to sensory input. From measurements of processing speed, grouping decisions within a particular cortical area are estimated to be reached within a few tens of milliseconds, implying that the selection mechanism is extremely fast and operates on the first spikes of responses[23]. Second, connections can contribute to grouping even if they are not directly activated by stimuli. Third, the ongoing activity patterns can be modulated by top-down influences. Thereby, attention and expectancy can be expressed in dynamic states and can contribute to fast grouping before stimuli have actually caused responses at higher processing stages.

Several arguments support such an interpretation. First, the preferential occurrence of latency covariations between cells with overlapping or similarly oriented RFs corresponds to the perceptual grouping criteria of vicinity and similarity. Second, the precise and column-specific latency covariations were restricted to states characterized by high gamma activity, and were related to excitability fluctuations in this frequency range. Gamma activity, in turn, is a signature of activated cortical states[24] and is commonly held to be a prerequisite of sensory processing in the cerebral cortex[25]. Third, self-generated, synchronized fluctuations of neuronal activity in the gamma frequency range in both humans and animals is associated with focused attention and the preparation of sensory–motor performance[26–30]. Taken together, this suggests that the notorious latency fluctuations of cortical responses to sensory stimuli may not be simply a reflection of noise and unreliable transmission, but rather, the consequence of a matching process between structured, self-generated activity and sensory signals that resembles a Bayesian operation. Through this matching process, the temporal coherence of responses would become adjusted as a function of structured excitability fluctuations that reflect the grouping rules residing in the functional architecture of cortico–cortical connections. As these fluctuations are also likely to be modulated by top-down influences and responses to preceding stimuli, they could serve as the dynamic expression not only of fixed network properties but also of predictions derived from stimulation history and centrally generated expectancies. Therefore, we propose that spontaneous activity and the resulting variability of responses should no longer be regarded as the result of noise, but rather as signatures of a dynamic coding process in which temporal relationships among discharge patterns are meaningful and contain information. In that case, suppression of response fluctuations by averaging may be inappropriate not only as a mechanism for 'noise' suppression in the nervous system but also as an experimental strategy in search of neuronal codes, because the potentially important information conveyed by covarying response fluctuations is averaged out.

METHODS

Preparation, recording and visual stimulation. All experimental procedures were in accordance with the German Law for the Protection of Experimental Animals and conformed with NIH and Society for Neuroscience regulations. Multi-neuron activity and local field potentials (LFPs) were recorded with 2 to 8 electrodes from 299 recording sites along 66 penetrations close to the representation of the area centralis from area 17 of 5 anesthetized (70% O_2/30% NO_2 supplemented by 0.4–0.8% halothane) and paralyzed (pancuronium, 10 mg/kg per h) cats and from 92 recording sites in area V4 of one awake fixating macaque monkey. For the analysis of neuronal spiking activity, the signals were band-pass filtered between 1 and 3 kHz and fed into Schmitt triggers that were set to at least twice the noise level. For the analysis of LFPs, signals were band-pass filtered between 1 and 100 Hz. Visual stimuli were presented on a computer screen at a frame rate of 100 Hz. The recorded neurons were characterized by plotting their RFs using computer-generated light bars and by compiling tuning curves for patches of moving sine wave gratings (0.5 cycles/degree, 2 degrees/s, full contrast). Tuning and preferred orientation were assessed using the vector averaging method[31]. A response was considered tuned if the ratio of the longest vector over the sum of all vectors was greater than 0.20. Relative overlap of RFs was quantitatively determined as the ratio of the overlap surface over the average of the two RF surfaces. RFs were considered to be (non-) overlapping if the overlap was (below) above 5%. Neurons at each recording site were stimulated with stationary flashed light bars (square wave grating with 1 cycle/degree and full contrast for the monkey recordings), with parameters (size, orientation and position) optimized to evoke maximal responses. For the assessment of latency covariations, an array of stimuli (one bar for each recording site, only one grating for all sites in the monkey) was presented repeatedly (100 to 300 times; stimulus duration, 2 s) with an intertrial interval of 15 s. A photodiode recorded stimulus onset with submillisecond precision.

Data analysis. Spike trains were first convoluted with a Gaussian (4 ms half width at half height) to generate a spike density function. The latency was defined with a precision of 0.1 ms as the time between stimulus onset and either the peak of the spike density function or the maximum of its derivative. Both measures gave the same results (Figs. 1 and 2) and, therefore, only data based on peak latencies are illustrated. Responses were accepted for latency measurements if the derivative of the average spike density function exceeded, within the first 70 ms (100 ms for the monkey V4 data) after stimulus onset and for at least three successive bins, the mean + 10 s.d. of the derivative of the spontaneous spike density function. Peaks of the spike density function or its derivative were accepted as latencies if they fell into a window from 5 ms before to 35 ms after the so-defined response onset. Latencies of LFP-predicted spike responses were determined following the same procedure as used for the single-trial latencies, except that the spike density functions were now averaged over 25 trials that were sorted according to LFP trajectories as indicated in Fig. 5a. Peak firing rates were assessed from the same spike density functions that were used to determine the latencies. For correlation analysis, we always used the non-parametric Spearman rank correlation coefficient. Fisher's Z-transform was used before correlation coefficients were averaged and the mean was retransformed. For the calculation of cross-power spectra of LFP signals, one-second sequences preceding stimulus onset were segmented into 20 overlapping intervals of 500 ms and hanning windowed. The cross-power spectra of these intervals were computed with a resolution of 2 Hz/bin using the FFT-algorithm. They were then averaged over the 20 segments to obtain single trial cross-power spectra, and these were then normalized and smoothed by convolution with a [1,3,3,1]-kernel.

ACKNOWLEDGEMENTS

Supported by the MPG and the Heisenberg program of the DFG. We thank S. Herculano-Houzel for suggestions, J.-H. Schröder and M. Stephan for help with data analysis, and J. Reynolds and R. Desimone for help in recording monkey data and for comments on the manuscript.

RECEVED 19 JULY; ACCEPTED 8 DECEMBER 2000

1. Arieli, A., Sterkin, A., Grinvald, A. & Aertsen, A. Dynamics of ongoing activity: explanation of the large variability in evoked cortical responses. *Science* 273, 1868–1871 (1996).
2. Gawne, T. J., Kjaer, T. W. & Richmond, B. J. Latency: another potential code for feature binding in striate cortex. *J. Neurophysiol.* 76, 1356–1360 (1996).
3. Gur, M., Beylin, A. & Snodderly, D. M. Response variability of neurons in primary visual cortex (V1) of alert monkeys. *J. Neurosci.* 17, 2914–2920 (1997).
4. Shadlen, M. N. & Newsome, W. T. The variable discharge of cortical neurons: implications for connectivity, computation, and information coding. *J. Neurosci.* 18, 3870–3896 (1998).
5. Alonso, J. M., Usrey, W. M. & Reid, R. C. Precisely correlated firing in cells of the lateral geniculate nucleus. *Nature* 383, 815–819 (1996).
6. Brecht, M., Singer, W. & Engel, A. K. Correlation analysis of corticotectal interactions in the cat visual system. *J. Neurophysiol.* 79, 2394–2407 (1998).
7. Singer, W. Neuronal synchrony: a versatile code for the definition of relations? *Neuron* 24, 49–65 (1999).
8. Tsodyks, M., Kenet, T., Grinvald, A. & Arieli, A. Linking spontaneous activity of single cortical neurons and the underlying functional architecture. *Science* 286, 1943–1946 (1999).
9. Lampl, I. & Yarom, Y. Subthreshold oscillations of the membrane potential: a functional synchronizing and timing device. *J. Neurophysiol.* 70, 2181–2186 (1993).
10. Volgushev, M., Chistiakova, M. & Singer, W. Modification of discharge patterns of neocortical neurons by induced oscillations of the membrane potential. *Neuroscience* 83, 15–25 (1998).
11. Nowak, L. G., Sanchez-Vives, M. V. & McCormick, D. A. Influence of low and high frequency inputs on spike timing in visual cortical neurons. *Cereb. Cortex* 7, 487–501 (1997).
12. Mainen, Z. F. & Sejnowski, T. J. Reliability of spike timing in neocortical neurons. *Science* 268, 1503–1506 (1995).
13. Stevens, C. F. & Zador, A. M. Input synchrony and the irregular firing of cortical neurons. *Nat. Neurosci.* 1, 210–217 (1998).
14. Azouz, R. & Gray, C. M. Cellular mechanisms contributing to response variability of cortical neurons in vivo. *J. Neurosci.* 19, 2209–2223 (1999).
15. Lampl, I., Reichova, I. & Ferster, D. Synchronous membrane potential fluctuations in neurons of the cat visual cortex. *Neuron* 22, 361–374 (1999).
16. Amzica, F. & Steriade, M. Short- and long-range neuronal synchronization of the slow (< 1 Hz) cortical oscillation. *J. Neurophysiol.* 73, 20–38 (1995).
17. Mitzdorf, U. Current source-density method and application in cat cerebral cortex: investigation of evoked potentials and EEG phenomena. *Physiol. Rev.* 65, 37–100 (1985).
18. Engel, A. K., König, P., Kreiter, A. K. & Singer, W. Interhemispheric synchronization of oscillatory neuronal responses in cat visual cortex. *Science* 252, 1177–1179 (1991).
19. Das, A. & Gilbert, C. D. Topography of contextual modulations mediated by short-range interactions in primary visual cortex. Nature 399, 655–661 (1999).
20. Schmidt, K. E., Kim, D. S., Singer, W., Bonhoeffer, T. & Löwel, S. Functional specificity of long-range intrinsic and interhemispheric connections in the visual cortex of strabismic cats. *J. Neurosci.* 17, 5480–5492 (1997).
21. Contreras, D. & Steriade, M. State-dependent fluctuations of low-frequency rhythms in corticothalamic networks. *Neuroscience* 76, 25–38 (1997).
22. Diesmann, M., Gewaltig, M. O. & Aertsen, A. Stable propagation of synchronous spiking in cortical neural networks. *Nature* 402, 529–533 (1999).
23. Thorpe, S., Fize, D. & Marlot, C. Speed of processing in the human visual system. *Nature* 381, 520–522 (1996).
24. Herculano-Houzel, S., Munk, M. H. J., Neuenschwander, S. & Singer, W. Precisely synchronized oscillatory firing patterns require electroencephalographic activation. *J. Neurosci.* 19, 3992–4010 (1999).
25. Makeig, S. & Jung, T. P. Tonic, phasic, and transient EEG correlates of auditory awareness in drowsiness. *Brain Res. Cogn. Brain Res.* 4, 15–25 (1996).
26. Bouyer, J. J., Montaron, M. F. & Rougeul, A. Fast fronto-parietal rhythms during combined focused attentive behaviour and immobility in cat: cortical and thalamic localizations. *Electroencephalogr. Clin. Neurophysiol.* 51, 244–252 (1981).
27. Sanes, J. N. & Donoghue, J. P. Oscillations in local field potentials of the primate motor cortex during voluntary movement. *Proc. Natl. Acad. Sci. USA* 90, 4470–4474 (1993).
28. Murthy, V. N. & Fetz, E. E. Oscillatory activity in sensorimotor cortex of awake monkeys: synchronization of local field potentials and relation to behavior. *J. Neurophysiol.* 76, 3949–3967 (1996).
29. Roelfsema, P. R., Engel, A. K., König, P. & Singer, W. Visuomotor integration is associated with zero time-lag synchronization among cortical areas. *Nature* 385, 157–161 (1997).
30. Fries, P., Reynolds, J. H., Rorie, A. E. & Desimone, R. Modulation of oscillatory neuronal synchronization by selective visual attention. *Science* (in press).
31. Swindale, N. V. Orientation tuning curves: empirical description and estimation of parameters. *Biol. Cybern.* 78, 45–56 (1998).